1-1-2015

A systematic approach to high and stable discharge capacity for scaling up the lithium-sulfur battery

Mohammad Rejaul Kaiser
University of Wollongong, mrk912@uowmail.edu.au

Jiazhao Wang
University of Wollongong, jiazhao@uow.edu.au

Xin Liang
University of Wollongong, xl475@uowmail.edu.au

Hua-Kun Liu
University of Wollongong, hua@uow.edu.au

Shi-Xue Dou
University of Wollongong, shi@uow.edu.au

A systematic approach to high and stable discharge capacity for scaling up the lithium-sulfur battery

Abstract

A systematic approach to improving the performance of the Li-S battery is presented, based on applying high energy ball milling to create a porous sulfur-carbon composite, insertion of a free-standing layer, and adoption of a new charging method. Surface area analysis and field emission scanning electron microscope imaging show that the ball-milled sulfur powder has a porous structure and very high specific surface area. A vacuum-filtrated single-walled carbon nanotube free-standing layer is inserted in between the sulfur cathode and the separator. It is believed that high-surface-area porous sulfur will help to increase the conductivity of the elemental sulfur due to better adhesion between the conducting carbon and the sulfur, while the free-standing layer will sequester longer chain polysulfides, which are responsible for the well-known shuttling phenomenon. By the combination of these methods, we have achieved excellent capacity and cycle life. Finally, a new charging method which will largely prevent the formation of longer chain polysulfides is also applied to increase the capacity retention. It is believed that with the combination of ball milling, the free-standing layer, and the new charging method, it is possible to commercialize the Li-S battery with better capacity and cycle life.

Disciplines

Engineering | Science and Technology Studies

Publication Details

Kaiser, M. Rejaul., Wang, J., Liang, X., Liu, H. & Dou, S. (2015). A systematic approach to high and stable discharge capacity for scaling up the lithium-sulfur battery. Journal of Power Sources, 279 231-237. Journal of Power Sources

A Systematic Approach to High and Stable Discharge Capacity for Scaling Up the Lithium-Sulfur Battery

Mohammad Rejaul Kaiser [a], Jiazhao Wang[a,*], Xin Liang[a], Hua-Kun Liu [a] and Shi-Xue Dou [a]

[a]Institute for Superconducting and Electronic Materials, University of Wollongong, Wollongong, NSW 2522, Australia

*Corresponding author, Tel: + 61 2 4298 1478; Fax: +61 2 4221 5731;
E-mail: jiazhao@uow.edu.au

Abstract

A systematic approach to improving the performance of the Li-S battery is presented, based on applying high energy ball milling to create a porous sulfur-carbon composite, insertion of a free-standing layer, and adoption of a new charging method. Surface area analysis and field emission scanning electron microscope imaging show that the ball-milled sulfur powder has a porous structure and very high specific surface area. A vacuum-filtrated single-walled carbon nanotube free-standing layer is inserted in between the sulfur cathode and the separator. It is believed that high-surface-area porous sulfur will help to increase the conductivity of the elemental sulfur due to better adhesion between the conducting carbon and the sulfur, while the free-standing layer will sequester longer chain polysulfides, which are responsible for the well-known shuttling phenomenon. By the combination of these methods, we have achieved excellent capacity and cycle life. Finally, a new charging method which will largely prevent the formation of longer chain polysulfides is also applied to increase the capacity retention. It is believed that with the combination of ball milling, the free-standing layer, and the new charging method, it is possible to commercialize the Li-S battery with better capacity and cycle life.

Keywords: Ball-milling parameters, Carbon sources, Free standing layer, Fixed capacity charging.

1. Introduction

With the advancement of portable electronics devices, electric cars, and hybrid electric vehicles, it is necessary to endow their energy storage devices with higher energy densities. Commercially available lithium-ion batteries exhibit specific energy of approximately 400 Wh/kg, which is inadequate for current needs [1]. Sulfur, which exhibits 2600 Wh/kg specific energy, could be a better option in terms of availability, cost, and performance, if it is possible to achieve high discharge capacity by reducing capacity fading and minimizing the insulating behavior. The latter problem can be minimized by using different types, shapes, and properties of conductive materials, specifically carbon-based materials [2]. Improving the discharge capacity, however, to near to the theoretical level and minimizing the capacity fading phenomenon are the burning questions that need to be solved, which involve solving the problems of polysulfide dissolution and the shuttling effect of polysulfide [3]. Extensive research has been conducted on different techniques: loading the sulfur onto carbon materials [4-9], engineering the cathode surface [10-12], using different electrolytes and binders [13, 14], and applying different additives, specifically conductive polymers [15, 16], to minimize the problems.

Previously published works on sulfur-carbon cathode material, where the sulfur was loaded either by melt diffusion or wet chemical precipitation [17-21], managed to achieve better specific capacity with allowable capacity fading, however, the synthesis methods that were adopted are complicated and laboratory oriented. To commercialize lithium sulfur batteries, it is important to develop a large-scale fabrication method for the production of S-C composites. Recently, Hui-Ming Cheng's group studied the large-scale fabrication of graphene-sulfur composites [19, 22] to obtain a high-performance long-life Li-S battery. In their work, they produced a unique Sulfur-graphene sandwich structure and managed to

achieve higher capacity retention. Their large-scale sulfur-graphene sandwich fabrication method is less facile and accessible, however, compared to the ball-milling method.

Ball milling is a simple, inexpensive, environmentally friendly, and industrially oriented method, which had been studied for mechanical mixing of materials for the Li-ion battery [23-26] since the beginning of the last decade. Moreover, this method is also extensively used in Li-ion battery research for manufacturing nanostructured materials [27], increasing reactivity [28], fabricating composites [29], and obviously improving rate capability and discharge capacity [30]. It has never been optimized, however, in terms of processing parameters and carbon sources for the Li-S battery. Sulfur and sulfur-carbon composites that were synthesized by un-optimized ball-milling processes failed to achieve higher specific capacity (even though they were better than commercial sulfur) and better capacity retention than with other synthesis methods [16, 31, 32], which makes them of less interest to the researcher.

Changing the physical and morphological characteristics of S-C composite is not the only way to improve the performance of the Li-S battery. The construction of the cell and the method of charging also play a pivotal role in better performance. A new approach has been established to improve cycling performance by inserting a free-standing carbon interlayer between the cathode and the separator [31-33]. With this new approach, it was possible to obtain 1400 to 1500 mAh/g initial discharge capacity, which is the maximum initial capacity that has been reported in the literature. By using that carbon layer, it was also possible to control capacity fading behavior. Jeong et al. [33] used an acetylene black free-standing layer and claimed that this free-standing layer acts as a fishing net that can capture polysulfide and inhibit the shuttle phenomenon. With the free-standing layer, they managed to reduce the capacity fading to 30-35% after 50 cycles.

On the other hand, very recently, Manthiram's group [34] achieved a breakthrough in the abatement of capacity fading by using a new charging method. With the help of that method, they managed to reduce capacity fading to as low as 1%. In their method, they charged the cell up to a certain capacity rather than using the conventional voltage window. They discovered that the first plateau of the discharge curve of sulfur, where the larger polysulfides (Li_2S_8, Li_2S_6) are formed, is responsible for the polysulfide dissolution and the shuttle phenomenon. So, they charged a Li-S cell up to a level such that the first plateau could not be formed and then allowed the cell to discharge. They found that the discharge capacity was almost equal to the charge capacity, which is definitely the maximum capacity retention for a Li-S battery ever recorded.

In this study, a systematic approach has been developed wherein a large-scale production method is used for the synthesis of S-C composite. In addition, a conductive single-walled carbon nanotube (SWCNT) free-standing layer with a refined, woven-like structure is inserted in between the cathode and the separator to improve the capacity and cyclability. This carbon layer was fabricated by ultrasonic dispersion followed by vacuum filtration [35]. Finally, the fixed capacity charging method was applied to improve the capacity retention.

2. Experimental

2.1. Synthesis of Carbon-Sulfur Composite: Commercial sulfur purchased from Sigma-Aldrich with 100 µm mesh size was used for ball milling in a planetary ball mill for different milling times (3, 6 and12 hours), at 100 rpm and with a 10:1 ball to sulfur weight ratio. Then, the ball-milled sulfur was morphologically, physically, and electrochemically characterized by FESEM, the Brunauer-Emmett-Teller (BET) technique, and battery testing with a Land automatic battery tester to find the best dwell time. The optimum dwell time, along with the best rotational speed and sample-to-ball weight ratio from the literature, was used for finding

the best carbon sources. Carbon black (CB), activated carbon (AC) and mesoporous carbon (MC) were ball milled with sulfur in a 30:70 weight ratio [36], and the resultant composites were denoted as carbon black–sulfur composite (CBS), activated carbon–sulfur composite (ACS), and mesoporous carbon–sulfur (MCS) composite.

2.2. Fabrication of SWCNT free-standing layer: 15 mg of SWCNT with 500 ml de-ionized water were poured into a beaker, and 500 mg of Triton-X100 surfactant was added. Then, the solution was probe sonicated for 1 hour with a 2 second pause time, followed by vacuum filtration and washing with de-ionized water and ethanol. The polytetrafluoroethylene (PTFE) filter paper with the SWCNT layer was dried under vacuum overnight at 60 ^{o}C, and finally, the SWCNT layer was easily peeled off from the filter paper [35]. Figure S4 shows the easy peeling of the FSL.

2.3. Fabrication of cells: For assembling the cells, we first prepared the cathode, which was based on carbon-sulfur composite, and the preparation method for all three carbon-sulfur composites was the same. The cathode was fabricated by using CBS/ACS/MCS, Super-P, and PVDF in an 80:10:10 ratio, which means that the active materials in the cathode amount to 56 wt% (70% × 80%). This mixture was manually mixed for 10 minutes, followed by mixing in a Kurabo MAZERUSTAR planetary mixer KK-250S for 15 minutes with the addition of N-methyl-2-pyrrolidone (NMP). The obtained slurry was coated on Al foil, and the coated Al foil was dried at 50 °C for 24 hours under vacuum. Then, the electrode was cut into 9.5 mm diameter discs, which were pressed at about 2 MPa. The fabricated disc electrodes were dried again at 50 °C for a few hours before use. The CR 2032 coin-type cells were assembled in an Ar-filled glove box where discs of Li foil were used as counter electrode and reference electrode. The electrolyte was prepared by dissolving 1 M LiTFSI and 0.1 M $LiNO_3$ in the co-solvents 1,3-dioxolane (DOL) and 1,2-dimethoxyethane (DME),

with a volume ratio of 1:1.A porous polypropylene film was used as the separator. The sequence of electrodes, electrolyte, separator, and FSL is shown in Figure S5.

2.4. Characterization: To characterize the ball-milled sulfur, carbon-sulfur composites, SWCNT free-standing layer, and Li-S cells, different analytical tools were used. For physical and morphological characterization of the ball-milled sulfur and carbon-sulfur composites, field emission scanning electron microscopy (SEM; JEOL FESEM-7500) and the 15 point N_2 absorption Brunauer-Emmett-Teller (BET) method on a Quanta Chrome Nova 1000 were used. For electrochemical performance evaluation of Li-S cells, an automatic battery tester system (Land®, China) was used at various current densities in the range of 1.5–3 V at room temperature.

3. Result and Discussion:

For the exploration of optimum processing parameters, such as the ball-to-sample weight ratio, the speed (rpm), and the dwell time in the ball-milling process is the first step in this systematic approach. These ball-milling parameters mainly depend on the physical properties of the pure sulfur [37]. To discover the most suitable parameters, an extensive literature survey was conducted, but it failed to find any papers that describe the ball milling of pure sulfur except for Takacs [38]. Among these three parameters, the ball-to-sample weight ratio and speed that were used in our work are 10:1 and 100 rpm, respectively, which are frequently used as ball milling parameters for other materials [23, 25, 39]. To determine the appropriate dwell time, which is one of the most important parameters for ball milling, we set the other two parameters as stated above and changed the dwell time to 3-hours, 6-hours, and 12-hours. The ball-milled sulfur was characterized physically, morphologically, and electrochemically to determine the most suitable dwell time.

Figure-1 shows the cycling performance of sulfur electrodes with different dwell times, where the electrode with 6-hours dwell time exhibits discharge capacity of 401.2 mAh/g after

fifty cycles, which is better than that of the other samples. Physical and morphological modification of sulfur due to different dwell time is the key factor for achieving better capacity. Figure S1 in the Supporting Information shows the morphological behavior of ball milled sulfur. Dwell time of 6 and 12 hours gives a smaller particle size and more porous structure than 0 hours (commercial sulfur) and 3 hours. Figure S1 also indicates that there is no significant difference between the results for dwell time of 6 and 12 hours except for slight agglomeration of the sulfur due to the higher dwell time. The morphological observations are also supported by Brunauer-Emmett-Teller (BET) testing, and the BET specific surface areas are presented in Table S1, where the dwell time of 6 hours gives the maximum specific surface area, followed by 12, 3 and 0 hours. It has been established that porous sulfur that shows higher specific surface area can confine carbon additives and inhibit shuttling behavior, resulting in better electrochemical performance [40]. From these results it can be deduced that 6-hours dwell time is the optimum parameter for the ball milling of sulfur, in combination with a 10:1 ball-to-sample weight ratio and 100 rpm speed.

After obtaining the optimum parameters for the ball milling of sulfur, our next step was to find the best carbon source among carbon black (CB), activated carbon (AC), and mesoporous carbon (MC) to manufacture carbon-sulfur composite, which is frequently used with sulfur for Li-S battery. It should be mentioned that for manufacturing carbon-sulfur composites, we used the ball-milling method with the optimized parameters that we determined in the first part, and the resultant composites are denoted as CBS, ACS, and MCS, respectively, which are described in Table 1. All these three carbons have very high specific surface area (> 500 m^2/g), but when they are coupled with sulfur, their surface area drops significantly due to confinement of carbon in the sulfur pores. Table 1 shows the specific surface areas of the three composites and that among them, the activated carbon–sulfur composite has the lowest specific surface area, followed by CBS and MCS. The lower

surface area of the composites is an indication of successful penetration of the carbon source into the sulfur pores. Figure 2 shows that submicron size AC flakes can easily penetrate the sulfur pores, and Figure S2 shows field emission SEM (FESEM) images of CBS and MCS composites where sulfur (yellow arrows) and carbons (red arrows) can easily be identified. MCS shows very low adhesion in between the carbon source and the sulfur, while on the other hand, CBS shows much better adhesion compared to MCS, but penetration of the carbon source into the sulfur pores is quite low. ACS, however, shows much more penetration of AC into the pores in the sulfur. From the FESEM image, we can infer that in ACS composite, the carbon is more confined by the sulfur due to the arbitrary size and shape of its particles than in the CBS and MCS composites. This result is also supported by the literature [2, 17], where it was reported that it is difficult to confine carbon black and mesoporous carbon in sulfur pores through a mechanical mixing process. To support the BET results and morphological analysis, and to find the best composite among these three, we conducted cycling performance and rate capability testing of these three composites, the results of which are shown in Figure 3.

The cycling results show that, the initial capacity of CBS is 1200 mAh/g, but it drops to 450 mAh/g after fifty cycles, which is about 34% of initial capacity. On the other hand, the initial capacity of ACS is 1172 mAh/g, and the capacity after fifty cycles is 698 mAh/g, which is about 60% of its initial capacity. Beside these two, MCS shows neither high initial capacity nor better capacity retention. The rate capability also indicates that CBS and ACS exhibit better performance at different current densities. It is notable that at higher current densities (2 C and 3 C), ACS shows much better capacity than CBS, which helped us to choose between these two composites for our next step. It can be inferred from the cycling performance that, the ACS composite is better than the other two in terms of capacity retention and higher current rates. Furthermore, it should be mentioned that neither the ball-

milled sulfur nor the carbon-sulfur composites show high discharge capacity and better capacity retention with respect to theoretical capacity. So, in the next phase, we will focus on the improvement of the capacity of ACS composite along with capacity retention.

To improve the initial capacity of the composite (ACS), we inserted a SWCNT free-standing layer (FSL) in between the separator and the cathode, which was fabricated through a vacuum filtration process. This approach was first introduced by Manthiram's group [31] by using multi-walled carbon nanotube (MWCNT) as a free-standing layer. Later, Kim [33] used acetylene black mesh as a FSL to capture dissolved polysulfide. Both of them managed to increase the initial capacity up-to 1450 mAh/g, but failed to achieve the theoretical capacity. This sort of FSL acts as a filter paper to trap the dissolved long chain polysulfides, preventing them from reaching the anode, and successfully reduces the polysulfide shuttle phenomenon. SWCNT, which has nanotubes with very small diameters (~10 nm), can form a woven-like structure that can act as a perfect filter paper for the filtration of polysulfide. Figure 4 shows the elemental mapping and quantitative analysis of the FSL after cycling, and it is clear that the sulfur is distributed homogeneously throughout the SWCNT free standing layer. Quantitative analysis shows that about 8% sulfur content is still present in the FSL after cycling, which is an indication of successful sequestering of longer chain polysulfide. There are two more peaks shown in the quantitative analysis, which belong to oxygen and fluorine. The fluorine comes from the polyvinylidene fluoride (PVDF) binder, and the oxygen comes from air.

To confirm the effects of the FSL, the cycling performance was examined with fixed and different current densities. Figure 5 (right) presents the discharge specific capacity of the sulfur composite with the FSL at different C-rates (1 C = 1675 mAh/g). By inserting the SWCNT FSL, we managed to achieve an initial capacity of 1674 mAh/g at 0.1 C, which is

the maximum capacity that has ever been reported for Li-S battery, and 1052 mAh/g was retained after fifty cycles. The FSL can improve the capacity not only at lower current density, but also at higher current density. It should be noted that the decrease in capacity does not have a linear relationship with increasing current density. It can be observed (Fig. 5) that at 3 C and 5 C, 700-800 mAh/g capacity is achieved, which is about half of the initial capacity at 0.1C. From Figure 5, we can also observe that although very high initial capacity has been achieved, the capacity retention is about 63% after fifty cycles, which means that the polysulfide dissolution problem was reduced to a certain extent, but the problem failed to be eradicated by using the SWCNT layer, which is a big hurdle for commercialization.

To improve the capacity retention, the new charging method developed by Manthiram's group [34] was followed, where the cells were charged up-to a certain capacity rather than using the conventional voltage window. It should be noted that the purpose of the new charging method is to prevent the formation of longer chain polysulfides that can be dissolved in the electrolyte and are responsible for the shuttle phenomenon. The longer chain polysulfides appear at the first plateau of the discharge curve, and to avoid that plateau, we must charge only up to a certain level where the first plateau cannot be formed. Manthiram's group found that the theoretical capacity of the 1^{st} and 2^{nd} plateau is 419 mAh/g and 1256 mAh/g, respectively. So, to get a stable capacity, it is necessary to charge the Li-S cell to lower than 1256 mAh/g, and for this purpose, we charged our cells at three different capacities (400, 600, and 800 mAh/g), which are lower than 1256 mAh/g, with 0.1 C current density and allowed them to discharge to observe the capacity retention. Figure 6 (top left) shows the cycling performance and voltage change with increasing cycle number. It is clearly demonstrated that the capacity retention is independent of the charge capacity, so long as it is under 1256 mAh/g, for ACS composite with FSL, and in this case, the retention is almost 99% after fifty cycles for the three different charge capacities that were used. The change in

voltage with cycle number is also significantly low, which indicates a very stable cycling performance. It should be noted that the deterioration of specific capacity is usually very intense for the first 20 or 50 cycles for any cells. If the capacity retention is not significantly reduced within this period, the cell is going to show higher capacity retention as cycling continues.

It can be concluded from the above discussion that the insertion of a SWCNT free-standing layer combined with the new charging technique can significantly improve the performance of the Li-S battery. Using the free-standing layer, however, will make the manufacturing process complicated and add to the cost. Therefore, we have tried to explore whether there is any possibility of only using the new charging technique to improve the capacity and cycling stability of commercial sulfur and ball-milled carbon-sulfur composite. Hence, we applied the new charging method to commercial sulfur and ball-milled carbon-sulfur composite; although unfortunately, the commercial sulfur failed to retain capacity, even at very low (~400 mAh/g) charge capacity. The voltage was varied frequently and eventually raised to over 3 V, where the capacity faded after a few cycles. The low capacity of the second plateau and the low initial discharge capacity are responsible for this. The ball-milled carbon-sulfur composite, however, showed quite stable discharge capacity at low (~500 mAh/g) charge capacity, but it was unstable at higher charge capacity compare to free standing layer contained ACS composite. Figure S3 shows the cycling performance of both commercial sulfur and ball-milled ACS composite with the fixed charging method, where the commercial sulfur and ACS composite show stable discharge capacity when charged to 300 mAh/g and 500 mAh/g, respectively. This result also confirms that the formation of porous sulfur via ball milling has a significant impact on the electrochemical properties. It can be inferred from the above discussion that the SWCNT free-standing layer helps to raise the initial capacity and to enlarge the second plateau to achieve better capacity retention at higher charge capacity.

4. Conclusion

It can be concluded that a systematic way of fabricating Li-S batteries that is suitable for large-scale production has been demonstrated by applying a series of facile methods (Figure S5). The fabrication of porous sulfur was achieved by the industrially-oriented ball-milling method, followed by identification of better carbon sources for that porous sulfur, by observing their physical, morphological, and electrochemical behavior. After that, the SWCNT free-standing layer was inserted to raise the discharge capacity of the best composite-the activated carbon–sulfur composite. By inserting the SWCNT free-standing layer, the initial capacity is raised to 1674 mAh/g, which is the maximum initial capacity recorded in the literature at this time. Finally, to retain the capacity for a higher number of cycles, a new charging method was applied, which helped to retain the capacity at about 99%. We believe that this method will help to make the Li-S battery commercially viable in the near future, representing a major advance for energy storage devices.

Acknowledgement

The authors gratefully acknowledge the financial support provided by Automotive Cooperative Research Centre (Auto CRC) and the support from the Institute for Superconducting and Electronic Materials (ISEM) and the Electron Microscopy Center (EMC) at the University of Wollongong. The authors also thank Dr. Tania Silver for critical reading of the manuscript.

References

[1] M. Armand, J.M. Tarascon, Nature, 451 (2008) 652-657.
[2] X. Ji, K.T. Lee, L.F. Nazar, Nat Mater, 8 (2009) 500-506.
[3] J. Zheng, M. Gu, M.J. Wagner, K.A. Hays, X. Li, J Electrochem Soc, 160 (2013) A1624-A1628.
[4] S. Moon, Y.H. Jung, W.K. Jung, D.S. Jung, J.W. Choi, D.K. Kim, Adv Mater, 25 (2013) 6547-6553.
[5] C. Zu, A. Manthiram, Advanced Energy Materials, 3 (2013) 1008-1012.
[6] L. Wang, Z. Dong, D. Wang, F. Zhang, J. Jin, Nano Lett, 13 (2013) 6244-6250.

[7] Z. Lin, Z.C. Liu, W.J. Fu, N.J. Dudney, C.D. Liang, Angew Chem Int Edit, 52 (2013) 7460-7463.
[8] L.W. Ji, M.M. Rao, S. Aloni, L. Wang, E.J. Cairns, Y.G. Zhang, Energ Environ Sci, 4 (2011) 5053-5059.
[9] K.P. Cai, M.K. Song, E.J. Cairns, Y.G. Zhang, Nano Lett, 12 (2012) 6474-6479.
[10] L. Wang, D. Wang, F. Zhang, J. Jin, Nano Lett, 13 (2013) 4206-4211.
[11] G. He, S. Evers, X. Liang, M. Cuisinier, A. Garsuch, L.F. Nazar, ACS Nano, 7 (2013) 10920-10930.
[12] C.S. Kim, A. Guerfi, P. Hovington, J. Trottier, C. Gagnon, F. Barray, A. Vijh, M. Armand, K. Zaghib, J Power Sources, 241 (2013) 554-559.
[13] M. Hagen, S. Dörfler, P. Fanz, T. Berger, R. Speck, J. Tübke, H. Althues, M.J. Hoffmann, C. Scherr, S. Kaskel, J Power Sources, 224 (2013) 260-268.
[14] K. Jeddi, K. Sarikhani, N.T. Qazvini, P. Chen, J Power Sources, 245 (2014) 656-662.
[15] M.-K. Song, Y. Zhang, E.J. Cairns, Nano Lett, 13 (2013) 5891-5899.
[16] G.-C. Li, G.-R. Li, S.-H. Ye, X.-P. Gao, Advanced Energy Materials, 2 (2012) 1238-1245.
[17] X. Li, Y. Cao, W. Qi, L.V. Saraf, J. Xiao, Z. Nie, J. Mietek, J.-G. Zhang, B. Schwenzer, J. Liu, J Mater Chem, 21 (2011) 16603-16610.
[18] W. Weng, V.G. Pol, K. Amine, Adv Mater, 25 (2013) 1608-1615.
[19] G. Zhou, S. Pei, L. Li, D.-W. Wang, S. Wang, K. Huang, L.-C. Yin, F. Li, H.-M. Cheng, Adv Mater, 26 (2014) 625-631.
[20] H.L. Wang, H.J. Dai, Chem Soc Rev, 42 (2013) 3088-3113.
[21] G.C. Li, J.J. Hu, G.R. Li, S.H. Ye, X.P. Gao, J Power Sources, 240 (2013) 598-605.
[22] G. Zhou, L.-C. Yin, D.-W. Wang, L. Li, S. Pei, I.R. Gentle, F. Li, H.-M. Cheng, ACS Nano, 7 (2013) 5367-5375.
[23] F. Gillot, M.P. Bichat, F. Favier, M. Morcrette, J.M. Tarascon, L. Monconduit, Ionics, 9 (2003) 71-76.
[24] D.-Y. Kim, M.-S. Song, J.-Y. Eom, H.-S. Kwon, J Alloy Compd, 542 (2012) 132-135.
[25] E. Panabière, N. Emery, S. Bach, J.P. Pereira-Ramos, P. Willmann, Electrochim Acta, 97 (2013) 393-397.
[26] Y.R. Jhan, J.G. Duh, J Power Sources, 198 (2012) 294-297.
[27] S.-B. Kim, S.-J. Kim, C.-H. Kim, W.-S. Kim, K.-W. Park, Mater Lett, 65 (2011) 3313-3316.
[28] Y.S. Jung, S. Lee, D. Ahn, A.C. Dillon, S.-H. Lee, J Power Sources, 188 (2009) 286-291.
[29] W.C. West, J. Soler, B.V. Ratnakumar, J Power Sources, 204 (2012) 200-204.
[30] S.R. Sivakkumar, A.S. Milev, A.G. Pandolfo, Electrochim Acta, 56 (2011) 9700-9706.
[31] Y.S. Su, A. Manthiram, Chem Commun, 48 (2012) 8817-8819.
[32] X.F. Wang, Z.X. Wang, L.Q. Chen, J Power Sources, 242 (2013) 65-69.
[33] T.-G. Jeong, Y.H. Moon, H.-H. Chun, H.S. Kim, B.W. Cho, Y.-T. Kim, Chem Commun, 49 (2013) 11107-11109.
[34] Y.S. Su, Y.Z. Fu, T. Cochell, A. Manthiram, Nat Commun, 4 (2013).
[35] S.Y. Chew, S.H. Ng, J.Z. Wang, P. Novak, F. Krumeich, S.L. Chou, J. Chen, H.K. Liu, Carbon, 47 (2009) 2976-2983.
[36] X. Zhao, D.-S. Kim, J. Manuel, K.-K. Cho, K.-W. Kim, H.-J. Ahn, J.-H. Ahn, J Mater Chem A, 2 (2014) 7265-7271.
[37] E. Gaffet, Materials Science and Engineering: A, 132 (1991) 181-193.
[38] L. Takacs, Journal of materials synthesis and processing, 8 (2000) 181-188.
[39] M. Lu, Y. Tian, Y. Yang, Electrochim Acta, 54 (2009) 6792-6796.

[40] D.-W. Wang, Q. Zeng, G. Zhou, L. Yin, F. Li, H.-M. Cheng, I.R. Gentle, G.Q.M. Lu, J Mater Chem A, 1 (2013) 9382-9394.

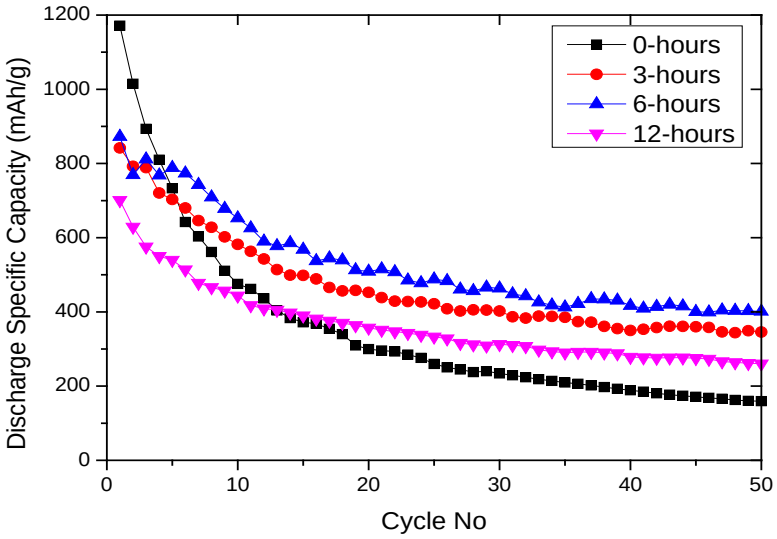

Figure 1: Cycling performance of ball-milled sulfur electrode with different dwell times.

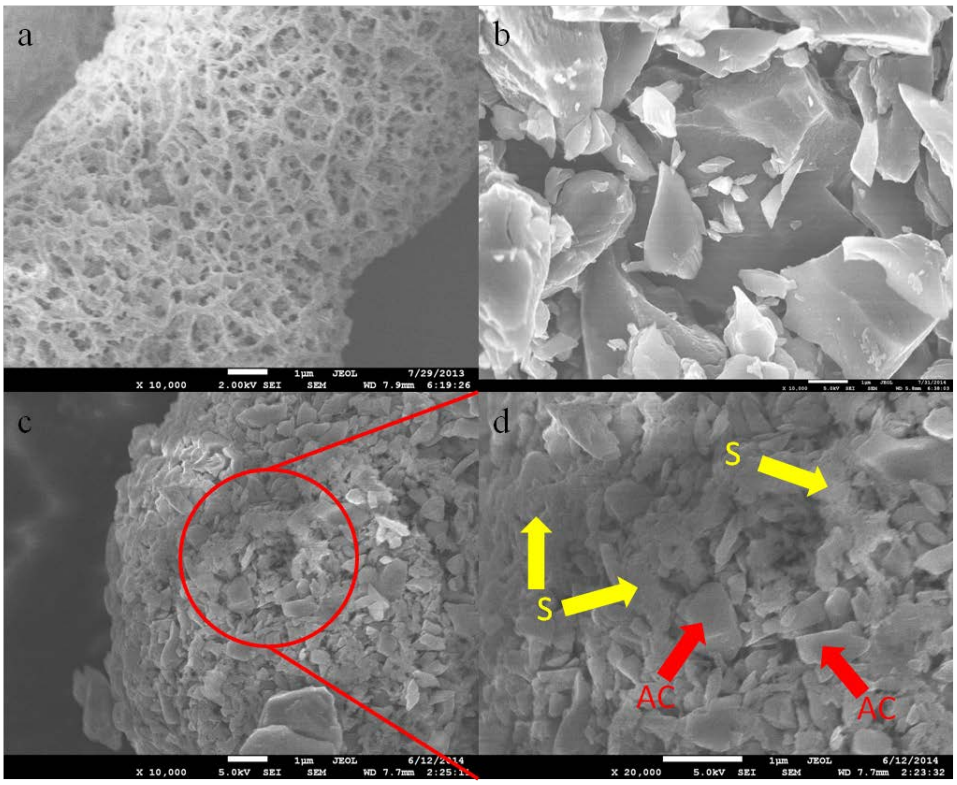

Figure 2: FESEM micrograph of a) pure sulfur (S), b) pure activated carbon (AC), c) & d) ball-milled ACS composite at different magnifications. The yellow arrows in (d) point the sulfur particles, and the red arrows point the activated carbon.

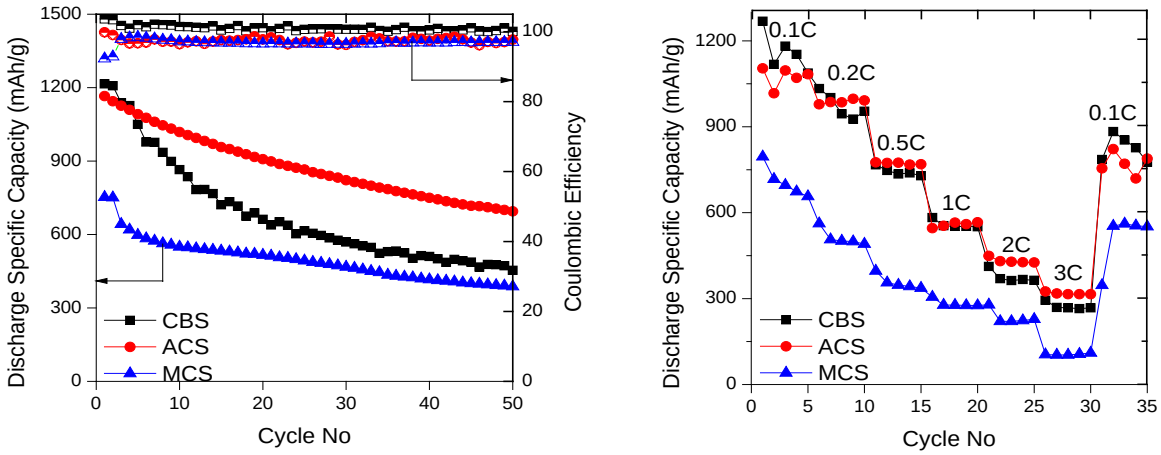

Figure 3: Cycling performance (left) and rate capability (right) of ball-milled carbon-sulfur composite.

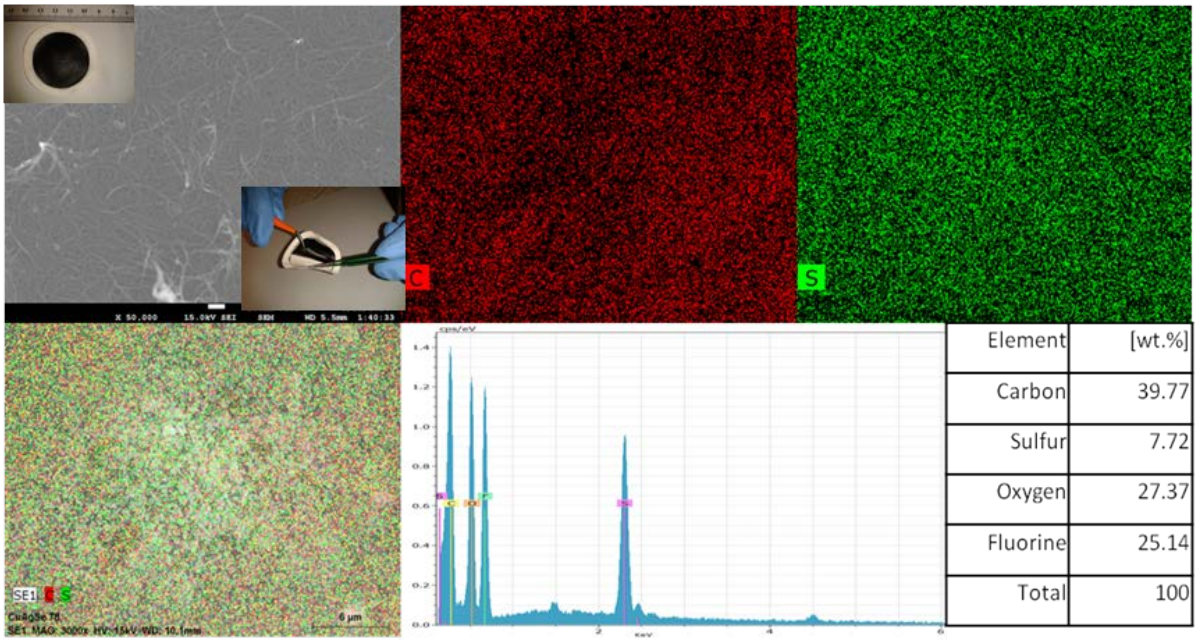

Figure 4: FESEM micrograph of SWCNT free standing layer before cycling (top left), with the insets showing photographs of the carbon interlayer, and energy dispersive spectroscopy (EDS) maps, spectrum, and elemental analysis of the carbon interlayer after cycling.

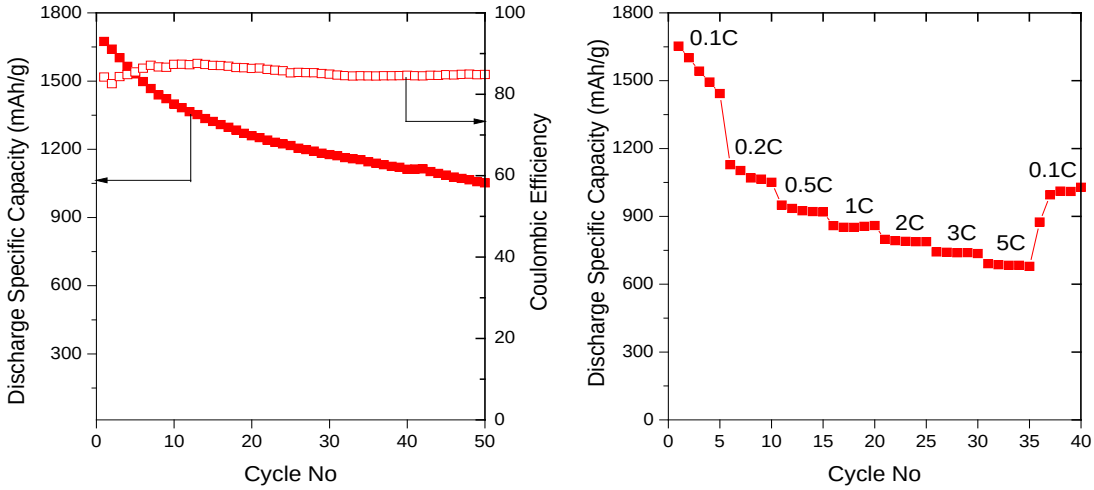

Figure 5: Cycling performance (left) and rate capability (right) of C-S composite with SWCNT free-standing layer.

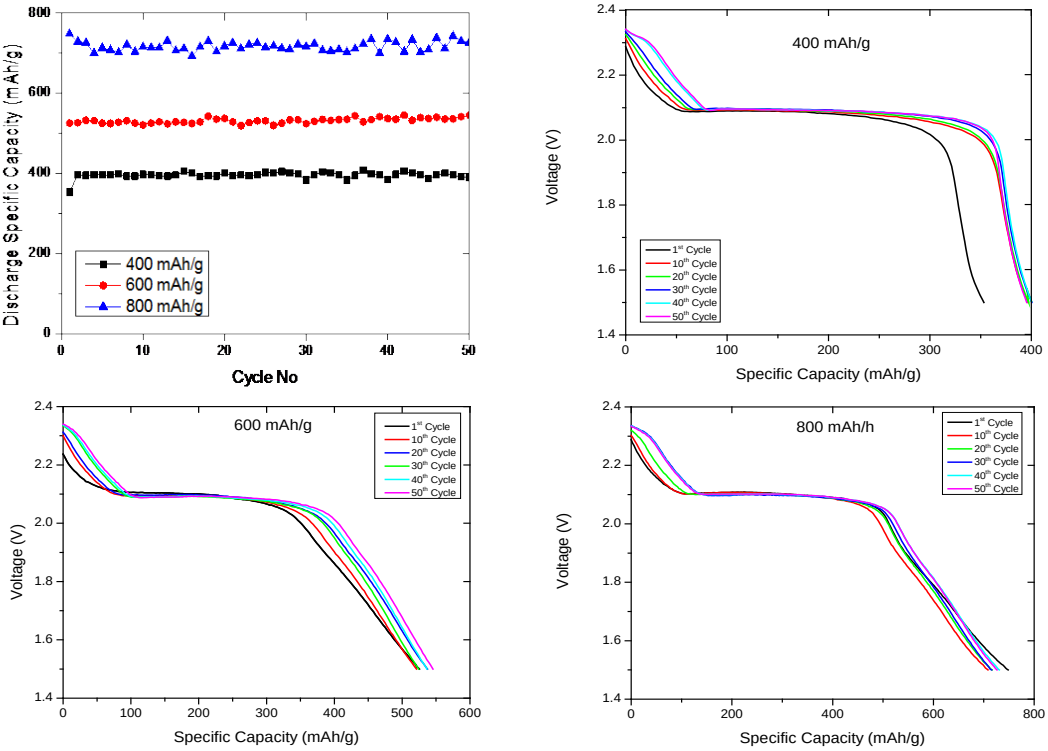

Figure 6: Fixed capacity cycling performance (top left) and voltage profiles for selected cycles of ACS with FSL at capacities limited to 400 mAh/g (top right), 600 mAh/g (bottom left), and 800 mAh/g (bottom right).

Tables:

Table 1: Specific surface areas (BET) of carbon-sulfur composites.

Sample Name	Denotation	Specific Surface Area (m^2/g)
Carbon Black–Sulfur Composite	CBS	16.05
Activated Carbon–Sulfur Composite	ACS	3.17
Mesoporous Carbon–Sulfur Composite	MCS	18.52

Supplementary Information

Correspondence and requests for materials: Jiazhao Wang (jiazhao@uow.edu.au)

A Systematic Approach to High and Stable Discharge Capacity for Scaling Up the Lithium-Sulfur Battery

Mohammad Rejaul Kaiser [a], Jiazhao Wang[a,*],Xin Liang[a], Hua-Kun Liu [a] and Shi-Xue Dou [a]

[a]Institute for Superconducting and Electronic Materials, University of Wollongong, Wollongong, NSW 2522, Australia

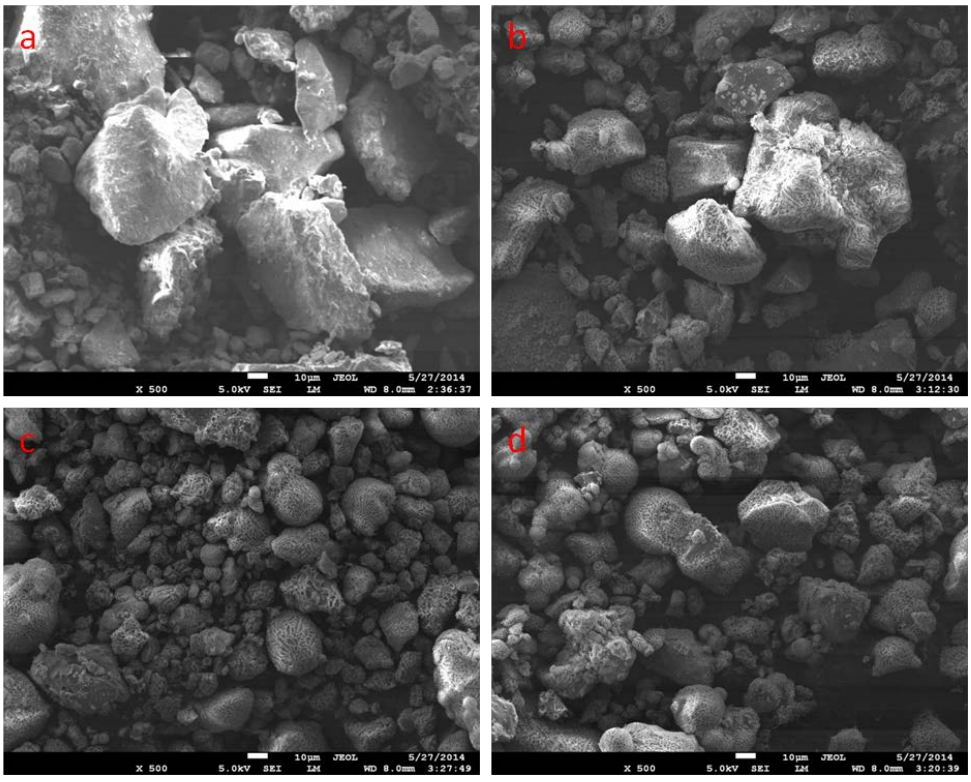

Figure S1: FESEM images of ball-milled sulfur after different dwell times: a) 0 hours, b) 3 hours, c) 6 hours, and d) 12 hours.

Table S1: Specific surface area (BET) against dwell time.

Dwell Time	Specific Surface Area (m^2/gm)
0 hours (commercial)	0.2637
3 hours	0.3190
6 hours	0.4346
12 hours	0.3202

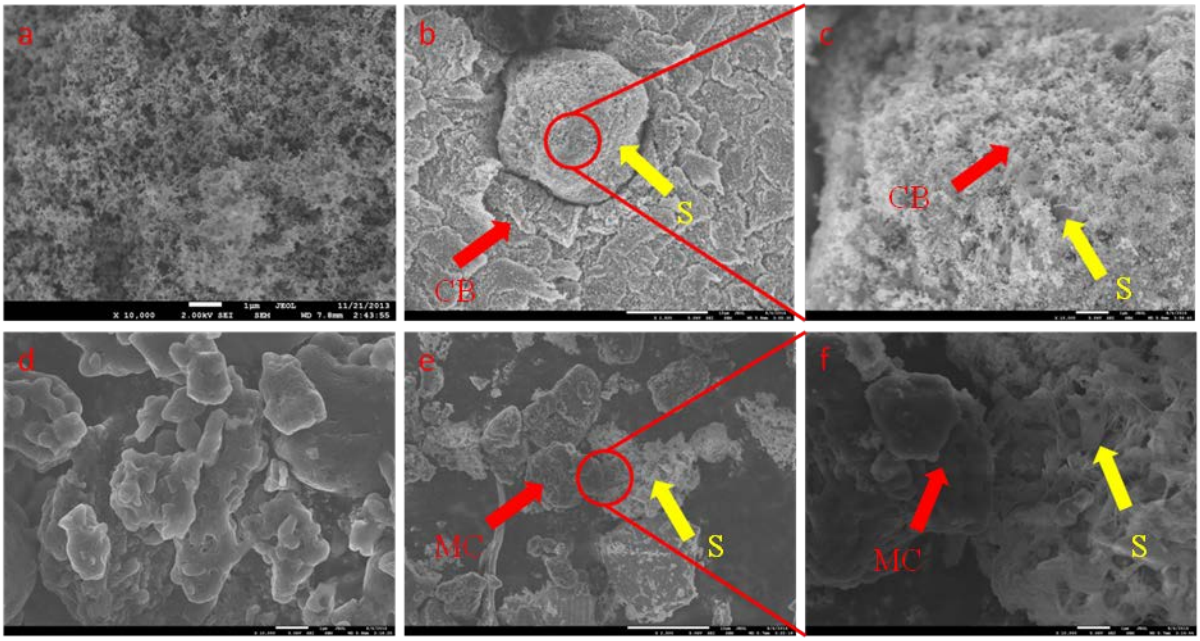

Figure S2: FESEM images of ball-milled carbon-sulfur composites: a) pure carbon black (CB), b) CBS (lower magnification), c) CBS (higher magnification), d) pure mesoporous carbon (MC), e) MCS (lower magnification) and f) MCS (higher magnification). The yellow arrows point the sulfur particles, and the red arrows point the carbon.

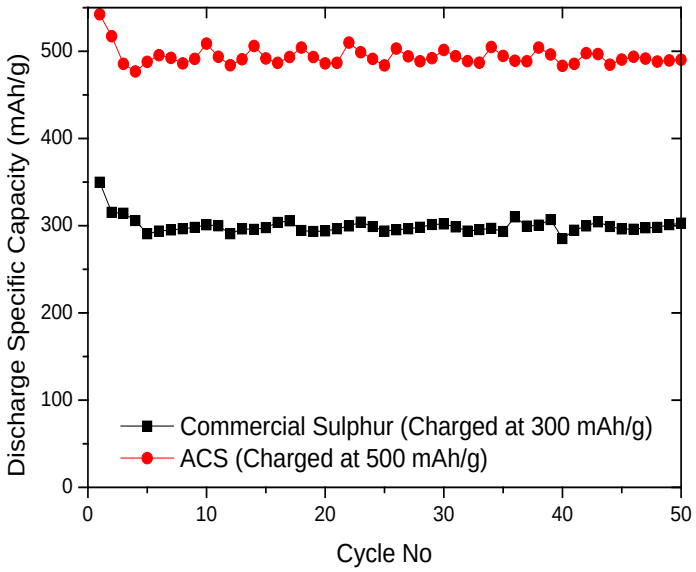

Figure S3: Cycling performances of commercial sulfur and ACS with fixed charge capacity.

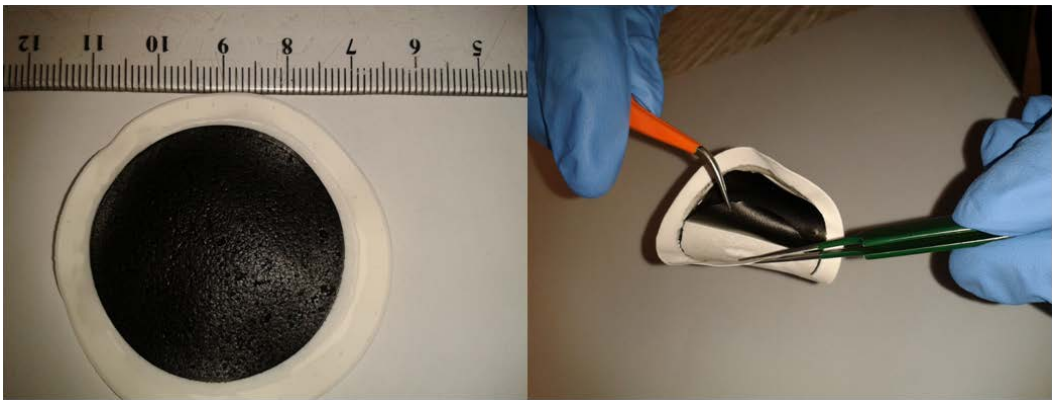

Figure S4: Easy peeling of FSL.

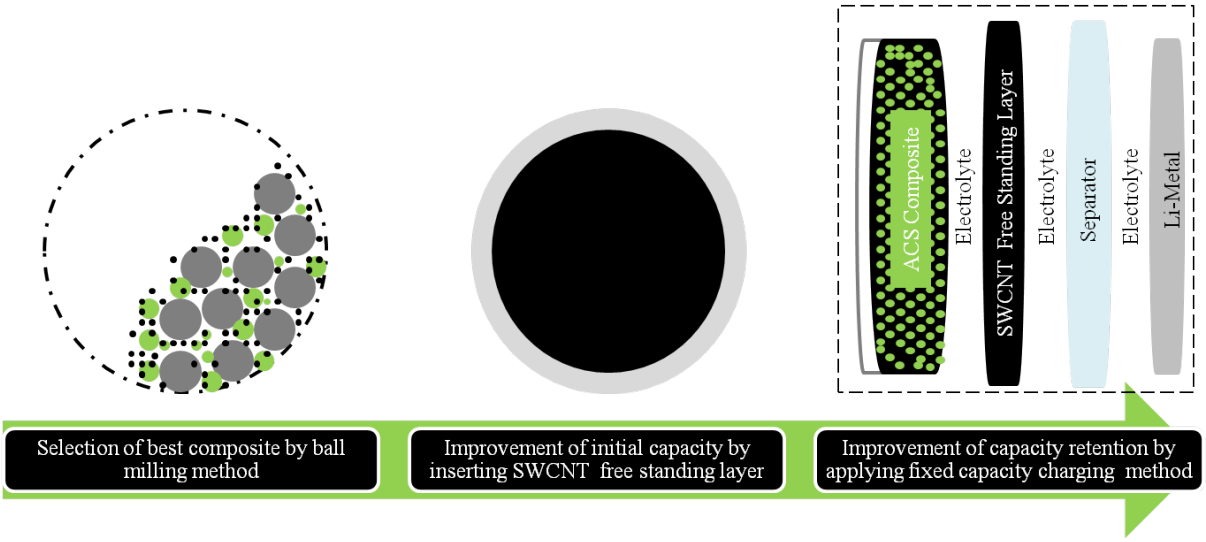

Figure S5: Systematic approach and structural sequence inside cell.